Comparison of Ceria-Supported Catalysts for Attaining NO - NO_2 Equilibrium at Industrial Nitric Acid Plant Conditions

Jithin Gopakumar[1], Albert Miro i Rovira[1], Bjørn Christian Enger[2], David Waller[3], Magnus Rønning[1*]

1.Norwegian University of Science and Technology (NTNU), Department of Chemical Engineering, Sem Sælands vei 4, NO-7491 Trondheim, Norway

2.SINTEF Industry, Kinetic, and Catalysis group, P.O. Box 4760 Torgarden, NO-7465 Trondheim, Norway

3.YARA Technology Center, Herøya Forskningspark, Bygg 92, Hydrovegen 67, NO-3936 Porsgrunn, Norway

[*]*Corresponding author, E-mail address: magnus.ronning@ntnu.no (M. Rønning)*

S1 *In-situ* production of NO_2

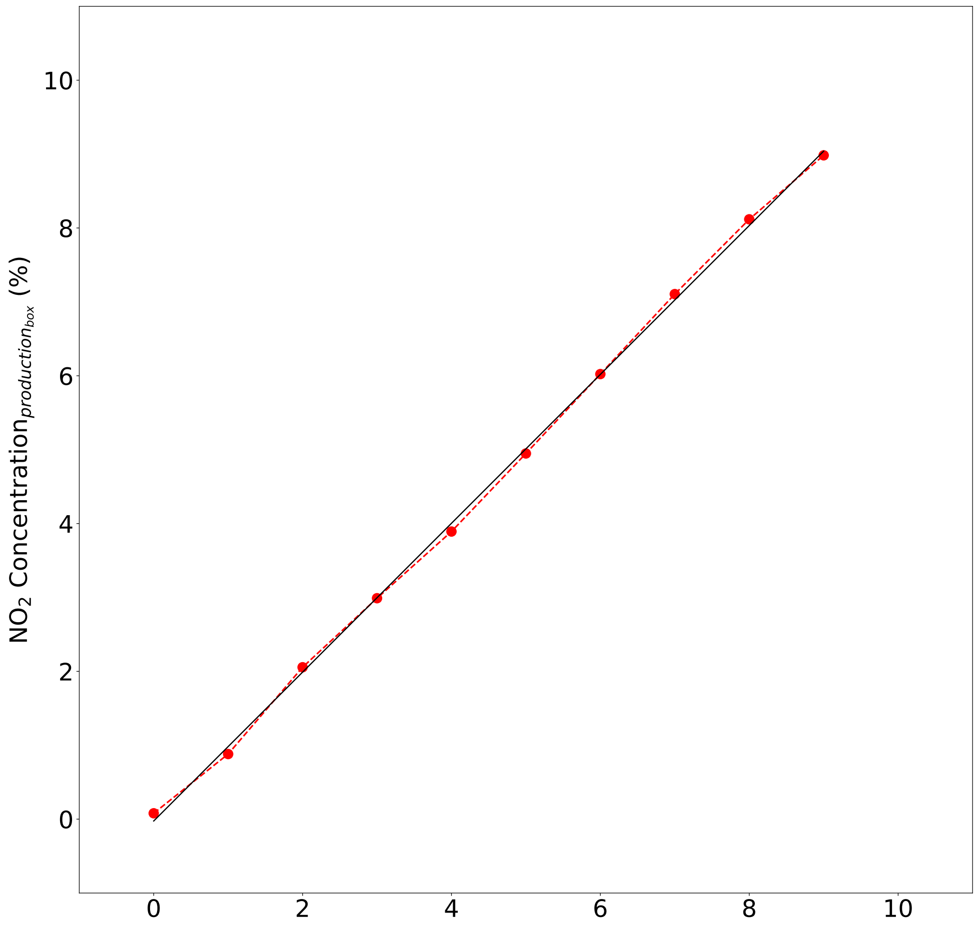

Figure S1: Parity plot between NO_2 concentration from production box versus 10%NO_2/Ar gas bottle. Note: This calibration was made at 150°C temperature and ambient pressure.

For activity measurements, all catalysts are subjected to two feed conditions with respect to temperature in the range of 150-400°C in this research work. Feed (ii) contains 2% NO_2 and as described in Section 2.3, NO_2 proportion increases with temperature and the ratio of N_2O_4 increases with pressure. To produce NO_2 *in-situ*, the empty reactor was heated to 150°C and calculated amounts of NO and O_2 were mixed close to NO_2 production box (presented in Fig. 2), the mixture reacts inside the production box. It travels through the empty reactor to the MKS FTIR, where NO_2 concentration is determined. A pre-calibrated mass spectrometer monitors O_2, N_2, and Ar in the feed. The set points for NO and O_2 were estimated when 100% NO to NO_2 conversion was achieved inside the box with no excess oxygen. The NO_2 production box consists of a 45cm 1/8" stainless steel tube (SS-316) connected from "a" to "b" points and surrounded by cooling water (presented in Fig. 2). A thermocouple (T3) is placed inside the box to monitor the water temperature during the reaction. NO_2 is produced at 25°C inside the production box. No notable changes in NO conversion were detected when the same experiment was conducted with the exit of NO_2 production box (point "b") directly connected to the analyser bypassing the reactor. The same experiment with 2%NO_2/Ar was repeated using NO_2 from 10%NO_2/Ar gas bottle and dedicated mass flow controllers (the results are presented in Fig. S1).

An empty reactor was heated from 150-450°C with 2%NO_2/Ar, no changes in NO_2 concentration were detected with respect to temperature (as seen in Fig. S2) in both ambient and 4bar pressures (inside the reactor). This simple *in-situ* production of NO_2 method can achieve higher concentrations of NO_2 which can be directly used for research to attain industrial concentrations of NO_x.

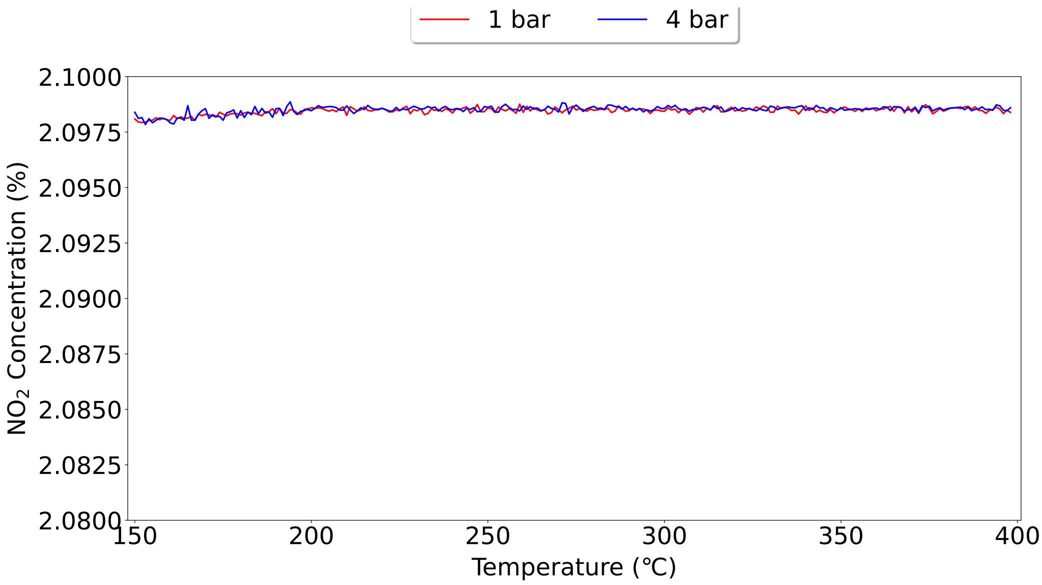

Figure S2: NO_2 concentration (%) as a function of temperature with 2% NO_2/Ar, heated at a rate of 5°C/min at WHSV= 24,000 $Ncm^3/g_{gcat}h$ at ambient and 4 bar pressure. Note: *In-situ* production is atmospheric, while the reactor was pressurised upto 4bar to record NO_2 concentration stabilisation.

S2 Chemisorption

Table S1 details the chemisorption program for the different catalysts.

Table S1: Chemisorption program for different ceria-based catalysts

Sample	**Pretreatment**[a] **Temperature**	**Reduction**[b] **Temperature**	**Pressure range [mmHg]**	**Isotherm Temperature**	**Adsorptive Gas**
Ag_{CeO_2}	450 °C	50 °C	30 – 500	50 °C	Hydrogen
Ru_{CeO_2}	120 °C	400 °C	30 – 500	35 °C	Carbon Monoxide
Ru_{Mn_5,CeO_2}	120 °C	400 °C	30 – 500	35 °C	Carbon Monoxide
$Ru_{Mn_{1}0,CeO_2}$	120 °C	400 °C	30 – 500	35 °C	Carbon Monoxide
$Ru_{Mn_{1}5,CeO_2}$	120 °C	400 °C	30 – 500	35 °C	Carbon Monoxide
$Ru_{Mn_{2}0,CeO_2}$	120 °C	400 °C	30 – 500	35 °C	Carbon Monoxide
Fe_{CeO_2}	450 °C	350 °C	30 – 500	50 °C	Hydrogen
Rh_{CeO_2}	400 °C	300 °C	30 – 500	35 °C	Hydrogen
Co_{CeO_2}	450 °C	350 °C	30 – 500	50 °C	Hydrogen
Ni_{CeO_2}	450 °C	450 °C	30 – 500	50 °C	Hydrogen
Au_{CeO_2}	450 °C	450 °C	30 – 500	50 °C	Hydrogen
Ir_{CeO_2}	120 °C	200 °C	30 – 500	35 °C	Carbon Monoxide
Pt_{CeO_2}	120 °C	200 °C	30 – 500	30 °C	Carbon Monoxide

a. Pretreatment was performed under Ar with a dwell time of 1 hour.

b. The reduction was performed at respective temperatures as mentioned with a dwell time of 2 hours.

S3 Catalytic conversion

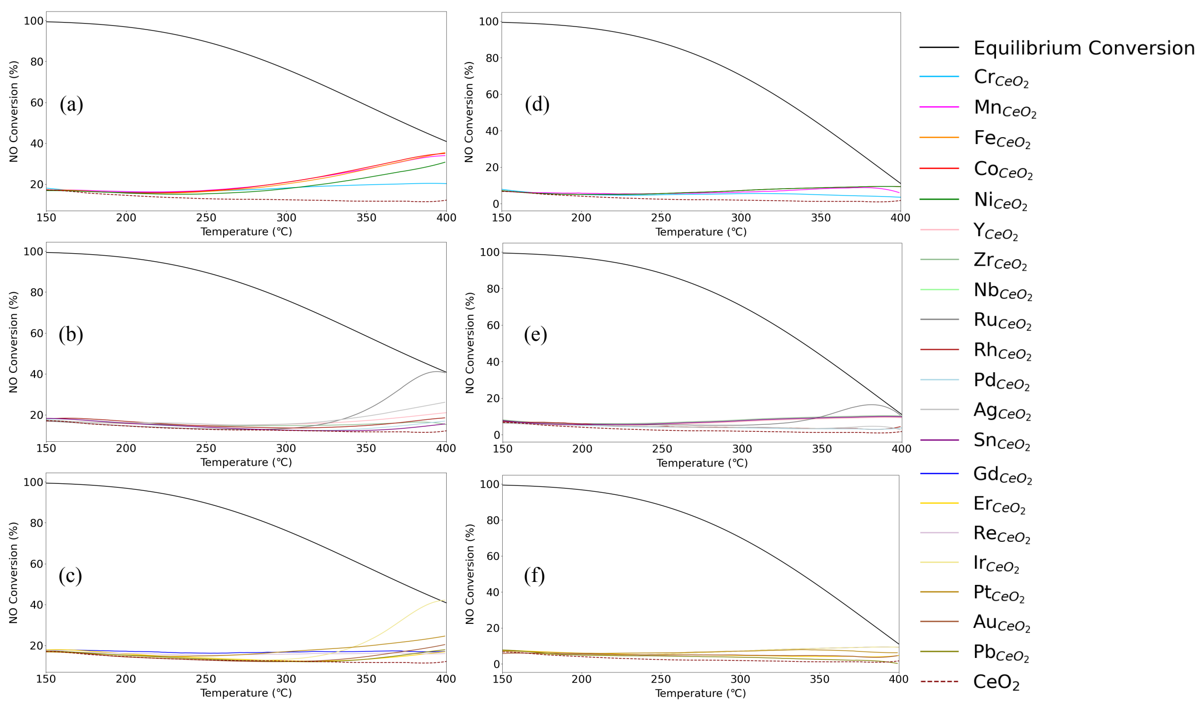

Figure S3: NO conversion (%) of (a) Period 4 mono-metallic catalysts, (b) Period 5 mono-metallic catalysts and (c) Period 6 mono-metallic catalysts in Feed (i): 10% NO, 6% O_2, 15% H_2O and rest Ar; (d) Period 4 mono-metallic catalysts, (e) Period 5 mono-metallic catalysts and (f) Period 6 mono-metallic catalysts in Feed (ii): 8% NO, 2% NO_2, 5% O_2, 15% H_2O and rest Ar as a function of temperature, heated at a rate of 5°C/min at WHSV= 24,000 $Ncm^3/g_{gcat}h$ at ambient pressure.

S4 X-ray diffraction plots

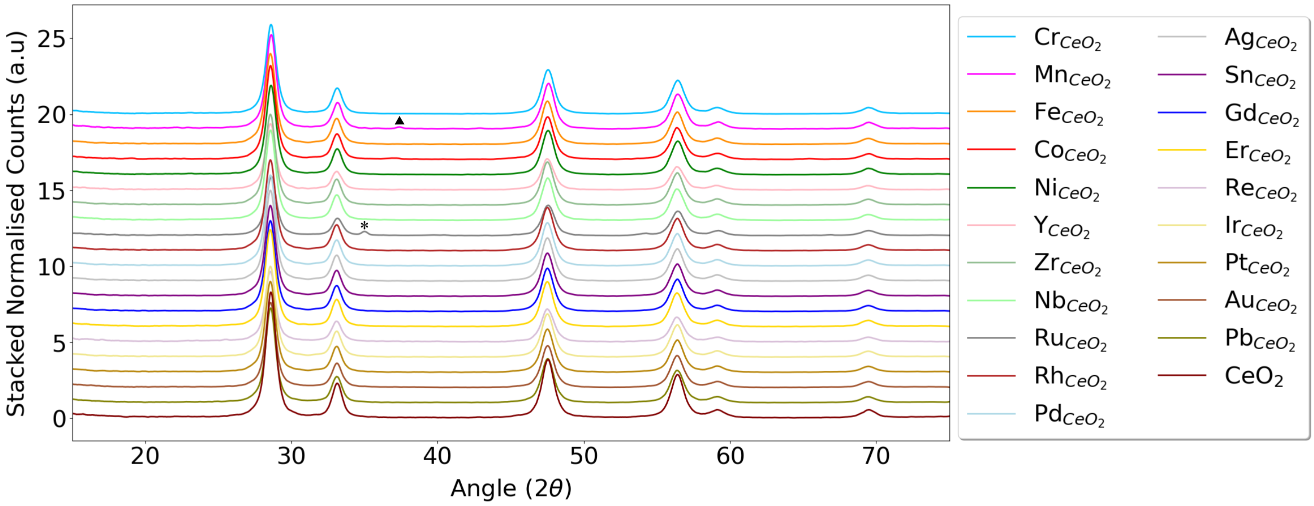

Figure S4: X-ray diffraction (XRD) patterns recorded for the CeO_2 support (PDF-00-034-0394), all mono-metallic catalyst samples in the 2θ range 5-75° with Cu K_α radiation (1.54060Å). Diffraction peaks of RuO_2 (PDF-04-003-2008) are represented as * and MnO_2 (PDF-04-007-3893) are presented as △

S5 Apparent activation energy

Table S2: Apparent activation energy (E_a) in two different feeds; Feed (i) 10% NO, 6% O_2, 15% H_2O and rest Ar and Feed (ii) 8% NO, 2% NO_2 5% O_2, 15% H_2O and rest Ar, with a space velocity of 24,000 $Ncm^3/g_{gcat}h$

Catalyst	**$E_a$feed(i)**[a]	**$R^2_{E_afeed(i)}$**	**$E_a$feed(ii)**[b]	**$R^2_{E_afeed(ii)}$**
Cr_{CeO_2}	11.6±0.62	0.9973	–	0.9979
Mn_{CeO_2}	30.9±0.51	0.9997	24.34±0.68	0.9956
Fe_{CeO_2}	37.9±0.42	0.9998	12.41±0.67	0.9973
Co_{CeO_2}	34.5±0.54	0.9997	12.42±0.62	0.9974
Ni_{CeO_2}	37.9±0.81	0.9995	12.73±0.39	0.9973
Y_{CeO_2}	36.9±0.49	0.9998	13.41±0.65	0.9973
Zr_{CeO_2}	27.9±0.83	0.9991	10.93±0.58	0.9974
Nb_{CeO_2}	52.2±0.92	0.9981	–	0.8968
Ru_{CeO_2}	117.8±0.61	0.9998	81.7±0.52	0.99968
Ru_{Mn_5,CeO_2}	47.0±0.81	0.9996	91.16±0.66	0.9997
Ru_{Mn_{10},CeO_2}	39.4±0.55	0.9999	85.39±0.91	0.9990
Ru_{Mn_{15},CeO_2}	54.9±0.98	0.9999	61.72±0.59	0.9996
Ru_{Mn_{20},CeO_2}	70.5±0.45	0.9998	57.85±1.57	0.9953
Rh_{CeO_2}	52.2±0.91	0.9981	–	0.896
Pd_{CeO_2}	118.5±0.94	0.9971	–	0.6989
Ag_{CeO_2}	49.8±0.76	0.9997	–	0.9641
Sn_{CeO_2}	96.5±11.1	0.9880	11.63±0.62	0.9973
Re_{CeO_2}	14.3±1.29	0.9925	12.45±0.68	0.9974
Ir_{CeO_2}	13.51±0.69	0.9998	13.51±0.69	0.9974
Pt_{CeO_2}	32.3±0.91	0.9988	–	-0.9152
Au_{CeO_2}	123.4±0.87	0.9992	–	-0.0109
Pb_{CeO_2}	162.6±0.98	0.9992	–	-0.9631
Gd_{CeO_2}	11.5±6.06	0.9925	12.46±0.67	0.9973
Er_{CeO_2}	118.5±1.52	0.9971	–	0.6988

a. The apparent activation energy was calculated using four parallel experiments with the same material. The Arrhenius plot fit is presented in Fig. S5.

b. The apparent activation energy was calculated using four parallel experiments with the same material. Some experiments did not lead to satisfactory Arrhenius plot fit in feed (ii) (presented in Fig. S6).

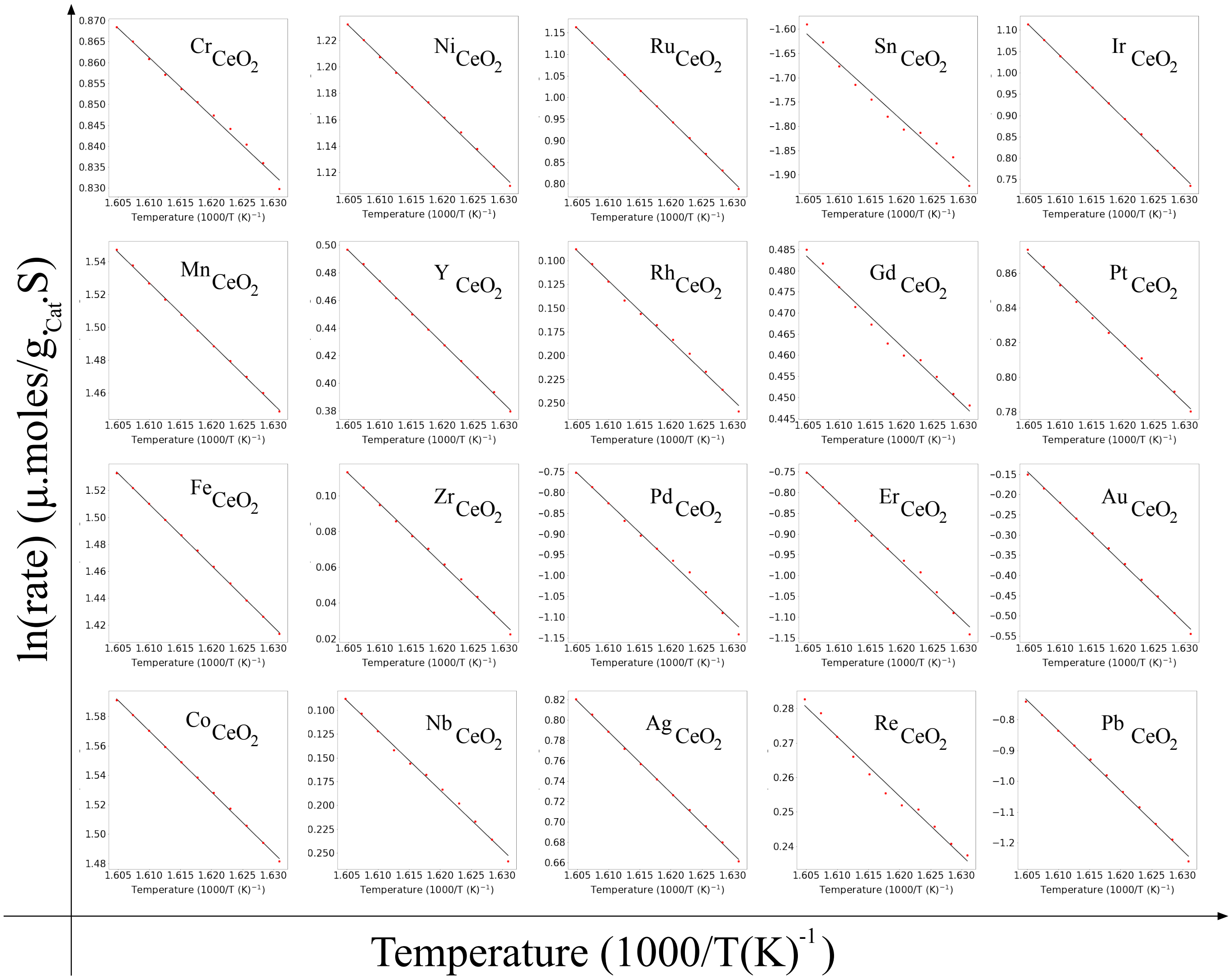

Figure S5: Arrhenius plot of the rate of NO oxidation to NO_2 on all mono-metallic catalysts as a function of temperature with Feed (i): 10% NO, 6% O_2, 15% H_2O and rest Ar, at WHSV= 24,000 $Ncm^3/g_{gcat}h$ at ambient pressure.

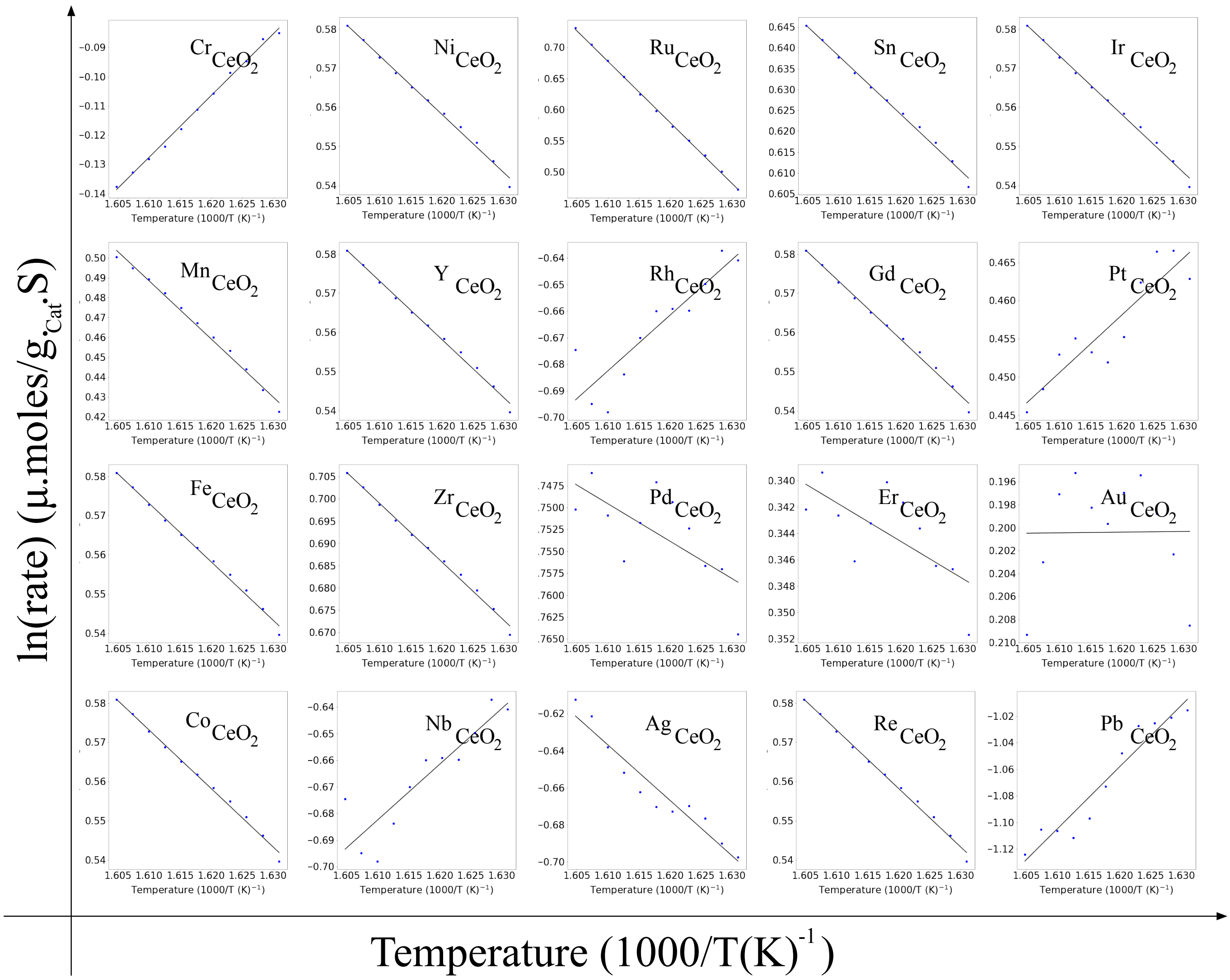

Figure S6: Arrhenius plot of the rate of NO oxidation to NO_2 on all mono-metallic catalysts as a function of temperature with Feed (ii): 8% NO, 2% NO_2, 5% O_2, 15% H_2O and rest Ar, at WHSV= 24,000 $Ncm^3/g_{gcat}h$ at ambient pressure.

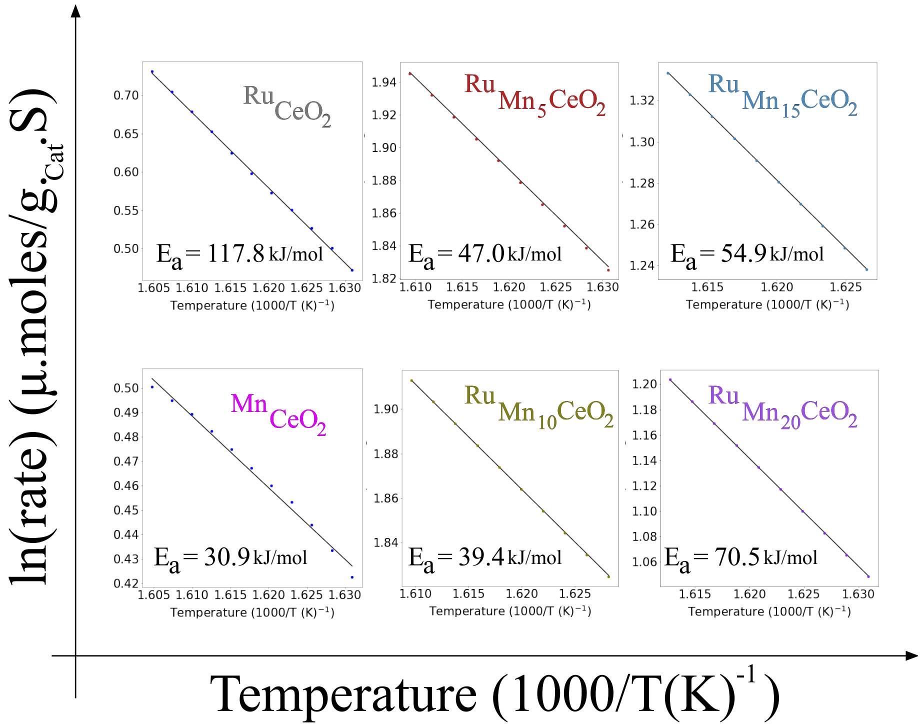

Figure S7: Arrhenius plot of the rate of NO oxidation to NO_2 on the monometallic Mn_{CeO_2} and Ru_{CeO_2} catalysts in comparison with bimetallic Ru_{Mn_5,CeO_2}, Ru_{Mn_{10},CeO_2}, Ru_{Mn_{15},CeO_2} and Ru_{Mn_{20},CeO_2} catalysts as a function of temperature with feed (i): 10% NO, 6% O_2, 15% H_2O and rest Ar, at WHSV= 24,000 $Ncm^3/g_{gcat}h$ at ambient pressure.

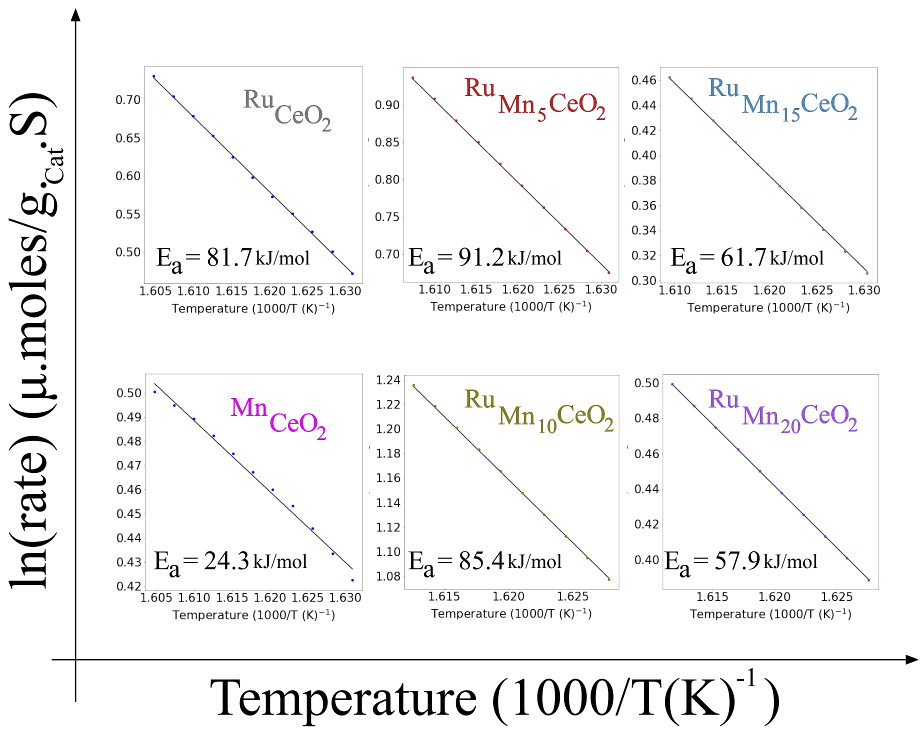

Figure S8: Arrhenius plot of the rate of NO oxidation to NO_2 on the monometallic Mn_{CeO_2} and Ru_{CeO_2} catalysts in comparison with bimetallic Ru_{Mn_5,CeO_2}, Ru_{Mn_{10},CeO_2}, Ru_{Mn_{15},CeO_2} and Ru_{Mn_{20},CeO_2} catalysts as a function of temperature with feed (ii): 8% NO, 2% NO_2, 5% O_2, 15% H_2O and rest Ar, at WHSV= 24,000 $Ncm^3/g_{gcat}h$ at ambient pressure.